

An ICT guided ratiometric naphthalene-benzothiazole based probe for detection of cyanide with real time application in human breast cancer cell

Shilpita Banerjee^a, Moumi Mandal^a, Satyajit Halder^b, Anirban Karak^a, Dipanjan Banik^a, Kuladip Jana^b, Ajit Kumar Mahapatra^{a*}

^aDepartment of Chemistry, Indian Institute of Engineering Science and Technology, Shibpur, Howrah 711 103, India

^bDivision of Molecular Medicine, Bose Institute, P 1/12, CIT Scheme VIIM, Kolkata-700 054, India.

*Author to whom correspondence should be addressed; electronic mail: akmahapatra@chem.iiests.ac.in; Tel.: +91 – 9434508013

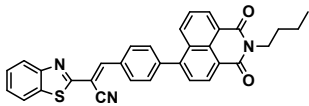
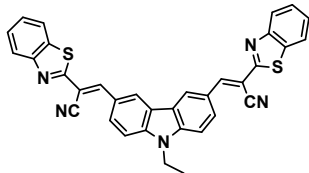
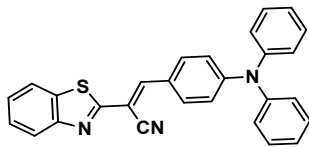
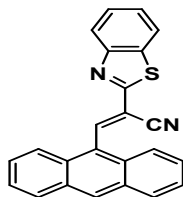
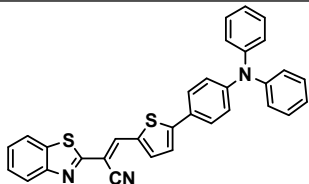
*Corresponding author. Fax: +91 33 26684564; Tel: +91 33 2668 4561;

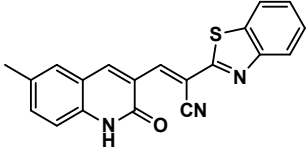
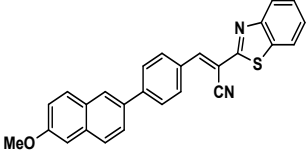
E-mail: mahapatra574@gmail.com (A. K. Mahapatra)

Table of Contents

Description	Page
1. Comparison table of previously reported cyanide sensors	3
2. Solid state cyanide sensing	4
3. Computational method	4
4. Live cell imaging study	5
5. Calculation of LOD	6
6. pH effect, application of the probe in tap and river water	7
7. Calculation of first order rate constant	8
8. Emission spectra of probe	9
9. Job's plot	9
10. Determination of Binding constant	10
11. NMR spectra of aldehyde, probe and product	10-11
12. Mass spectra of probe and product	12

1. Table S1 Comparison between previously reported CN⁻ sensors (based upon benzothiazole acetonitrile) with the current work

Sl. No.	Probe structure	Solvent	Sensor type	LOD	Application	Reference
1.		THF	Turn on (AIE)	$3.35 \times 10^{-5} \text{M}$	-	Choi et al., Spec acta A, 2021, 252, 119535
2.		DMSO	Turn on	3.73nM	-	Mondal et al., J of Luminescence, 2018, 201, 419-426
3.		Acetonitrile	Turn off	9.44ppm	Test strips	Qu et al., Sens & act B, 2017, 241, 1043-1049
4.		Acetonitrile	Ratiometric and turn on	$5.52 \times 10^{-8} \text{M}$ $2.35 \times 10^{-8} \text{M}$ $9.26 \times 10^{-8} \text{M}$	-	Chellappa et al., Sens & act B, 2017, 242, 434-442
5.		Acetonitrile	Turn on	$4.23 \times 10^{-8} \text{M}$	-	Nagamani et al., SN app sc, 2020, 2, 1069
6.		DMSO	Ratiometric	1 ppb	Sample water, test strips	Kumar et al., J of Mol Structure, 2022, 1250,

						131677
7.		DMSO	Ratiometric	$2.1 \times 10^{-8} \text{M}$	Environmental water samples, Test strips	This work

2. Solid state CN^- sensing:

Small piece of TLC sticks were dipped into $1 \times 10^{-5} \text{M}$ probe solution followed by drying in open air. The sticks were further dipped into two different concentrated solutions of CN^- ($1 \mu\text{M}$, $2 \mu\text{M}$) and dried for 5 minutes. After that photographs were taken to examine the sensing behaviour of the probe MNBTZ.

3. Computational method:

Theoretical calculations:

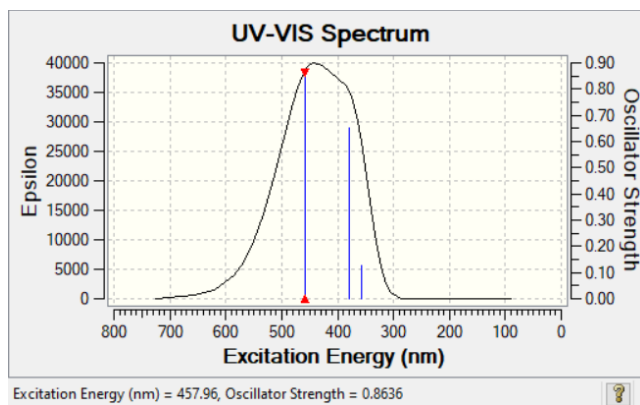


Figure S1. Absorption spectra of the Probe (MNBTZ)

Table S2The vertical main orbital transition of the **MNBTZ** calculated by TDDFT method

Energy(eV)	Wavelength (nm)	Osc. strength(f)	Transition
2.7073	457.96	0.8636	HOMO→LUMO
3.6081	379.05	0.6493	HOMO-1→LUMO
3.4677	357.54	0.1274	HOMO-2→LUMO

4. Live cell imaging study:

Cytotoxicity assay:

MTT cell proliferation assay was performed to assess the cytotoxic effect of the ligand **MNBTZ** in both the cancer cell line MDA-MB-231 and normal cell line NKE. In brief, cells were first seeded in 96-well plates at a concentration of 1×10^4 cells per well for 24 h and exposed to the different working concentration of ligand **MNBTZ** in DMSO and water ratio of 1:1(0 μ M, 10 μ M, 20 μ M, 40 μ M, 80 μ M, 100 Mm) for 24 hrs. After incubation cells were washed with 1 \times PBS and MTT solution (0.5 mg/ml) were added to each well and incubated for 4 hour and the resulting formazan crystals were dissolved in DMSO and the absorbance was measured at 570 nm by using a microplate reader. Cell viability was expressed as a percentage of the control experimental setup.

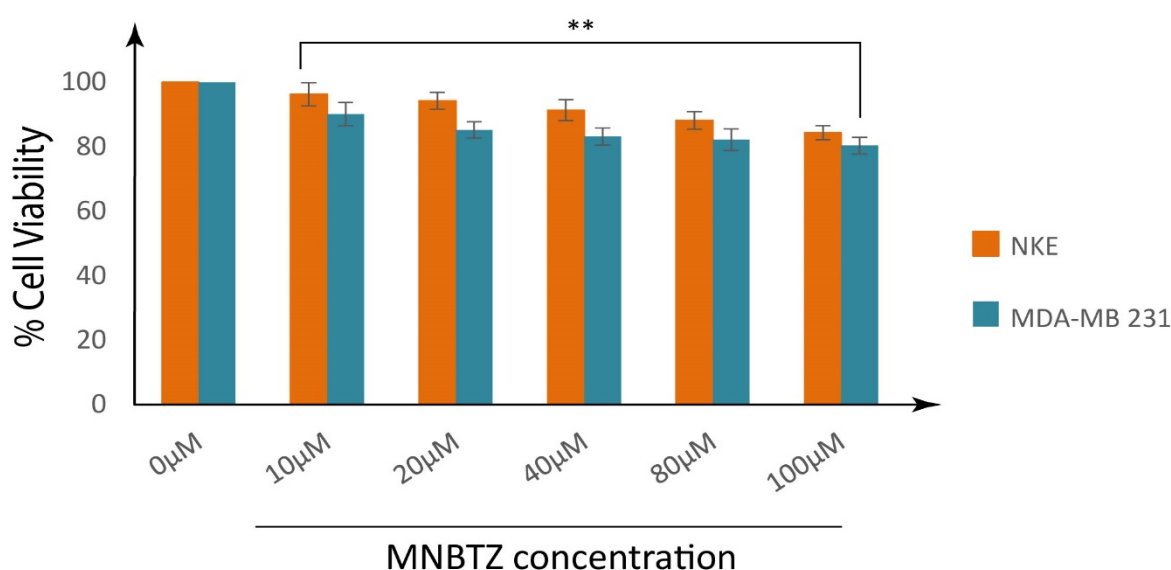


Figure S2. Cell survivability of MDA-MB 231 and NKE cells exposed to different ligand **MNBTZ** concentration. Data are representative of at least three independent experiments and bar graph shows mean \pm SEM, $**p < 0.001$ were interpreted as statistically significant, as compared with the control.

5. Calculation of Limit of detection:

From the plot of fluorescence intensity ratio I_{435}/I_{567} vs concentration of CN^- limit of detection was calculated by using the formula $LOD = k \times \delta / m$ where $k = 3$, δ is the standard deviation of the blank solution and m is the slope of the calibration curve.

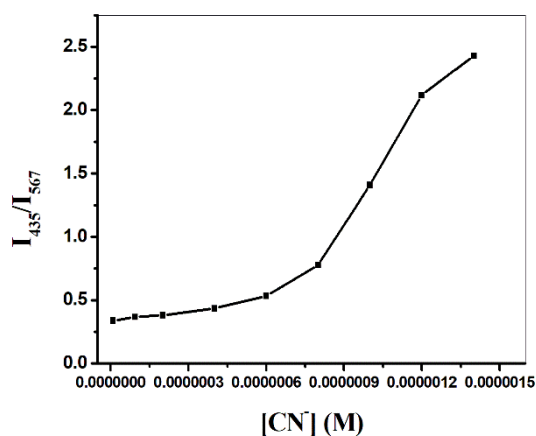


Figure S3. Plot of fluorescence intensity ratio vs concentration of CN^-

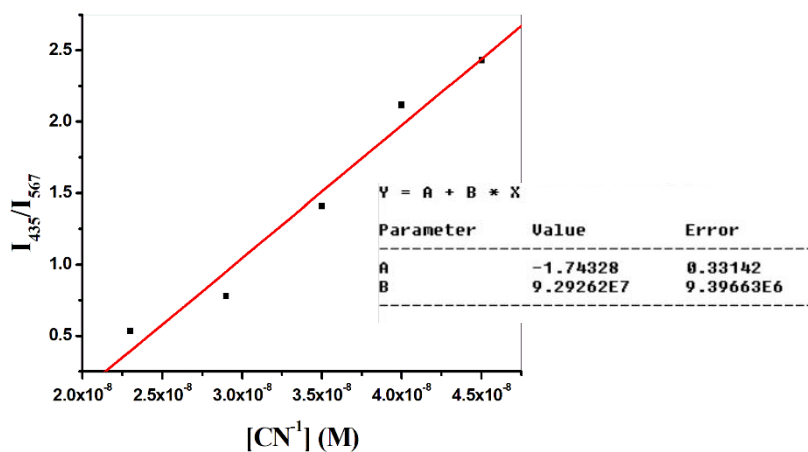


Figure S4. Calibration of the probe at an intensity ratio I_{435}/I_{567} depending on CN^- concentration.

LOD= 2.1×10^{-8} (M) ($R^2=0.98501$)

6.pH effect:

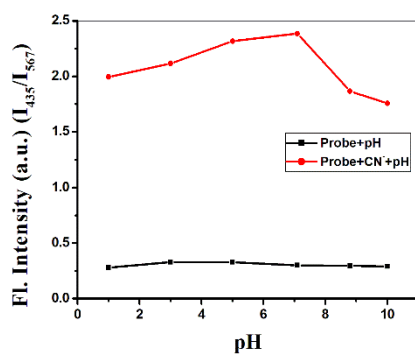


Figure S5. Effect of pH on fluorescence of MNBTZ and MNBTZ+ CN^- in DMSO/ H_2O at 380nm

7. Application of the probe in tap water and river water:

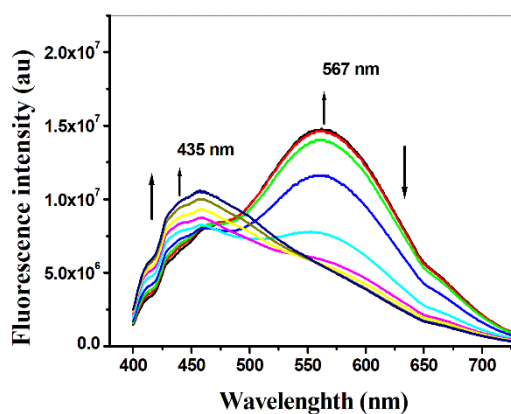


Figure S6: Fluorescence intensity changes of MNBTZ ($1 \times 10^{-5} \text{M}$) upon gradual addition of TBACN in **DMSO-tap water** ($10 \mu\text{M}$ HEPES buffer, 1:1 v/v, pH 7.4 at 25°C) ($\lambda_{\text{ex}}=380\text{nm}$, $\lambda_{\text{em}}=400\text{nm}$)

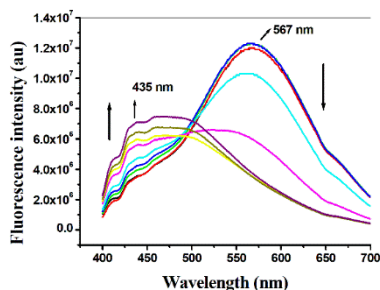


Figure S7: Fluorescence intensity changes of MNBTZ ($1 \times 10^{-5} \text{M}$) upon gradual addition of TBACN in **DMSO-river water** ($10 \mu\text{M}$ HEPES buffer, 1:1 v/v, pH 7.4 at 25°C) ($\lambda_{\text{ex}}=380\text{nm}$, $\lambda_{\text{em}}=400\text{nm}$)

Table S3: Real sample study for MNBTZ

Samples	Spiked(μM)	Found (μM)	Actual concentration of CN ⁻ in sample water (mg/L)
Tap water	30	30.216	0.09
River water	30	30.448	0.187

8. Calculation of first order rate constant (k')

First order rate constant was calculated by the following equation:

$$\ln[(F_{\text{max}} - F_t)/F_{\text{max}}] = -k't$$

Where F_t and F_{max} symbolize the fluorescence intensities at 435nm at time t and maximum value obtained upon completion of the reaction and k' is the monitored first order rate constant.

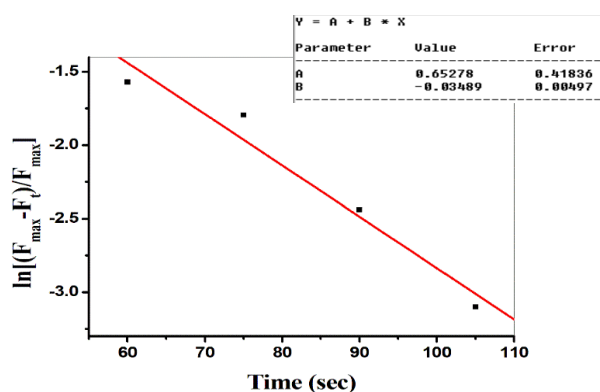


Figure S8. First order kinetic plot of probe ($1 \times 10^{-5} \text{M}$) in the presence of 2 equivalent of $1 \times 10^{-4} \text{M}$ CN^- solution ($\lambda_{\text{ex}}=380 \text{nm}$, $\lambda_{\text{em}}=400 \text{nm}$)

First order rate constant $k' = 0.0348 \text{ s}^{-1}$

9. Emission spectra of probe

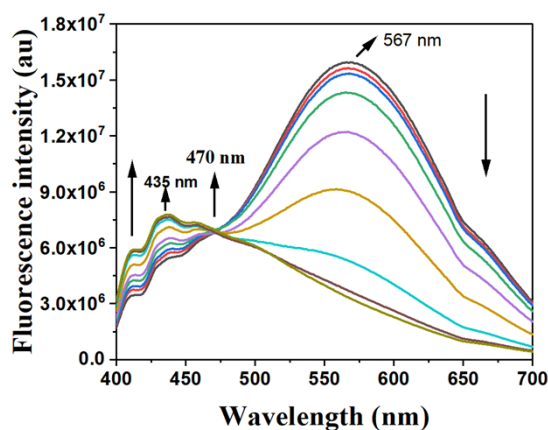


Figure S9. Fluorescence intensity changes of MNBTZ ($1 \times 10^{-5} \text{M}$) upon gradual addition of TBACN in **DMSO-distilled water** ($10 \mu\text{M}$ HEPES buffer, 1:1 v/v, pH 7.4 at 25°C) ($\lambda_{\text{ex}}=380 \text{nm}$, $\lambda_{\text{em}}=400 \text{nm}$)

10. Job's plot of the probe MNBTZ for CN^-

Job's plots were drawn by plotting $\Delta F \cdot X(\text{host})$ vs $X(\text{host})$ (ΔF = change of intensity ratio of the emission spectrum [I_{435}/I_{567}] for MNBTZ during titration and $X(\text{host})$ is the mole fraction of the host in each case respectively).

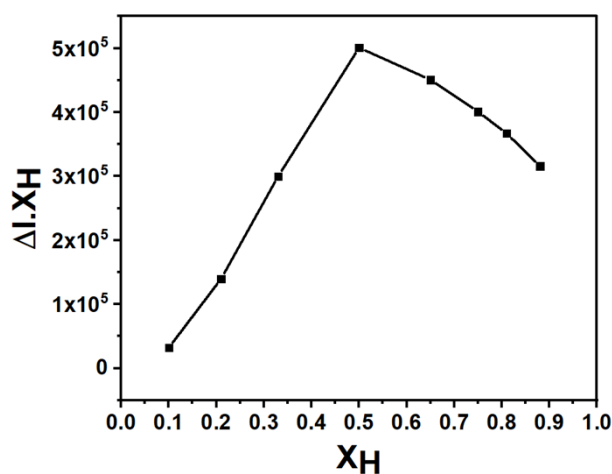


Figure S10. Job's plot of MNBTZ with CN^- using fluorescence data

11. Determination of binding constant value (K_a) using linear method for MNBTZ

Binding constant value (K_a) was calculated by plotting $1/\Delta I$ vs $1/[G]$ [(ΔI = change of intensity ratio of the emission spectrum [I_{435}/I_{567}] for MNBTZ during titration and $[G]$ is the concentration of CN^- in each case respectively).

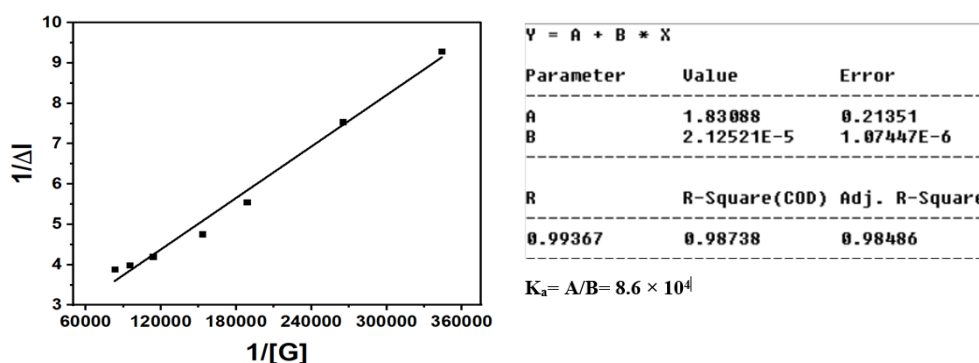


Figure S11. Binding constant value of MNBTZ with CN^- using fluorescence data

12. NMR spectra: ^1H -NMR, ^{13}C -NMR

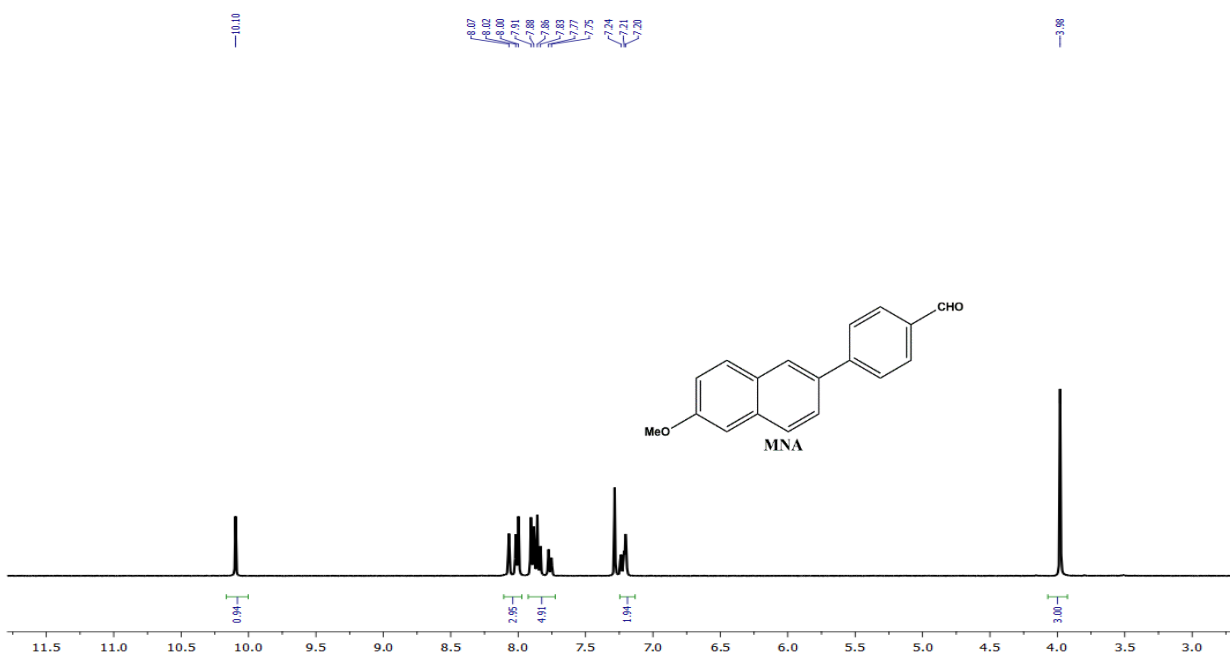


Figure S12: ^1H -NMR spectra of MNA in CDCl_3

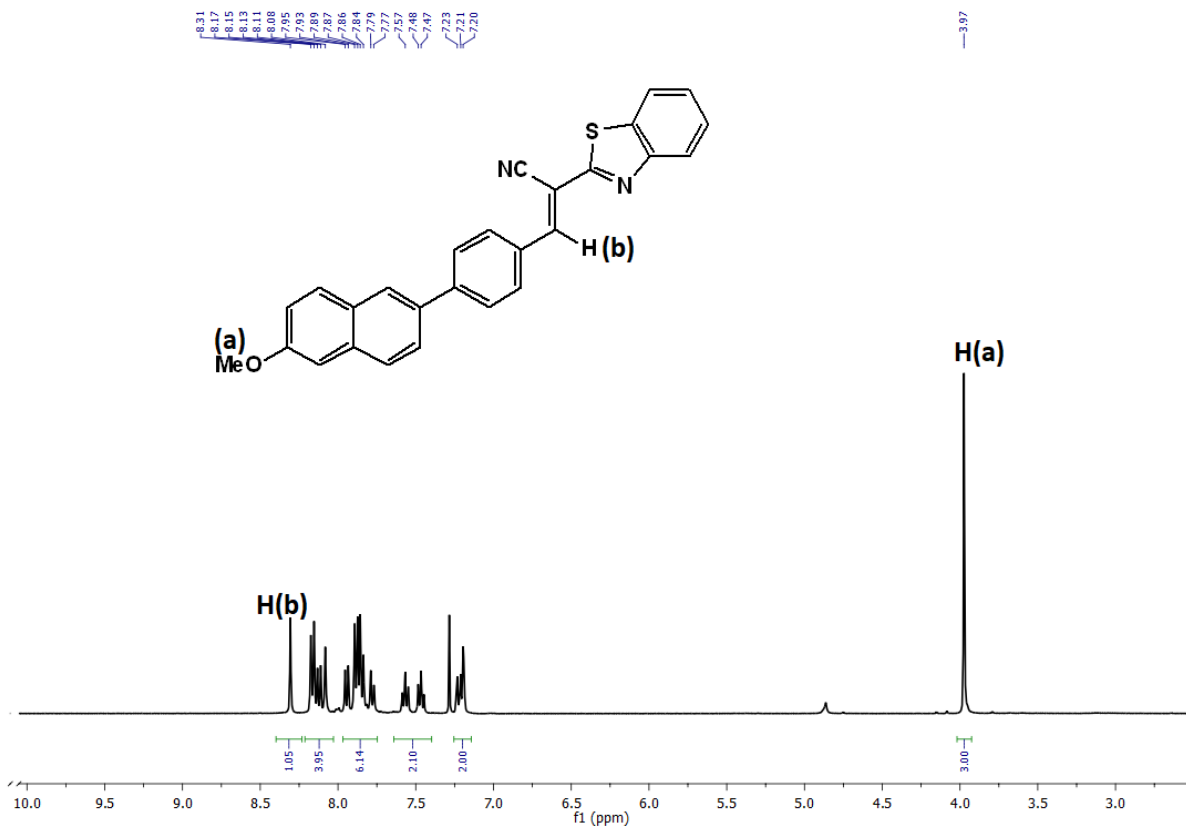


Figure S13: $^1\text{H-NMR}$ spectra of MNBTZ in CDCl_3

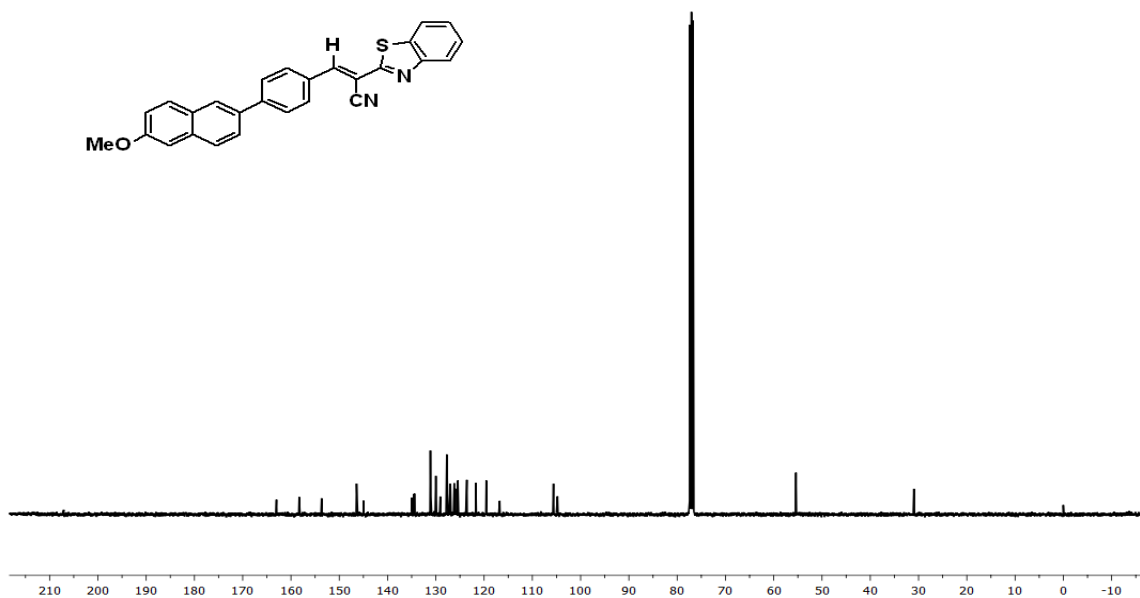


Figure S14: $^{13}\text{C-NMR}$ spectra of MNBTZ in CDCl_3

13. ESI-MS spectra

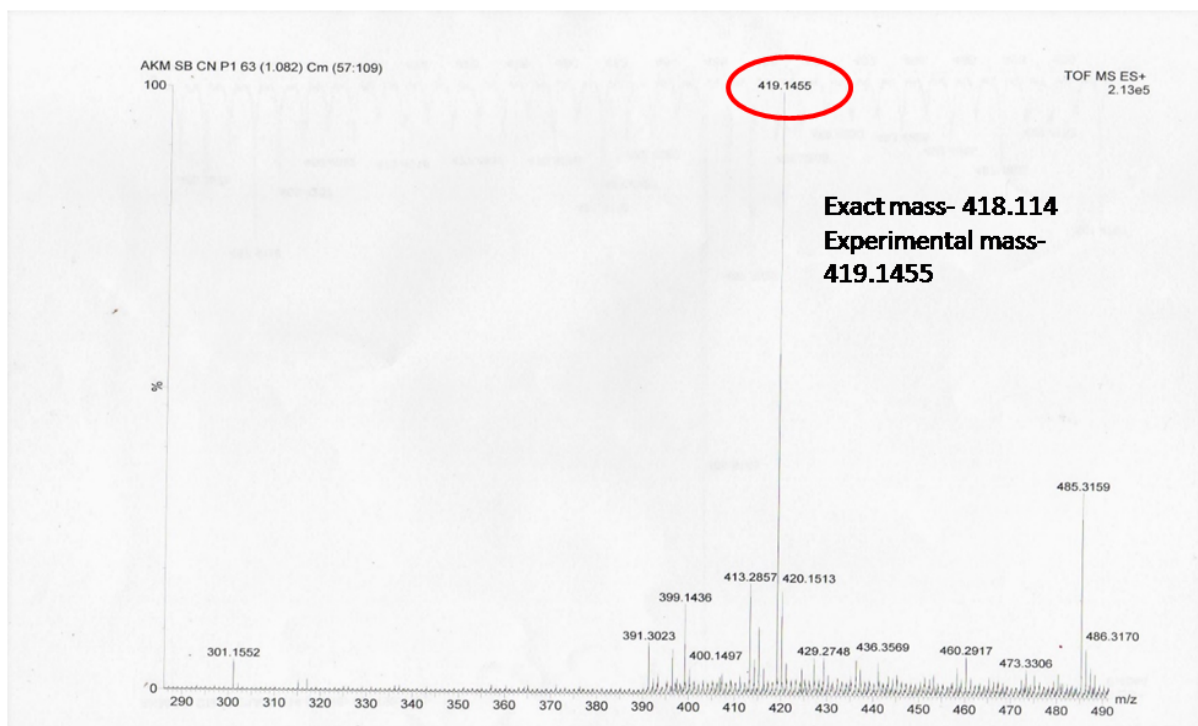


Figure S15: ESI-MS of probe MNBTZ [M+H]

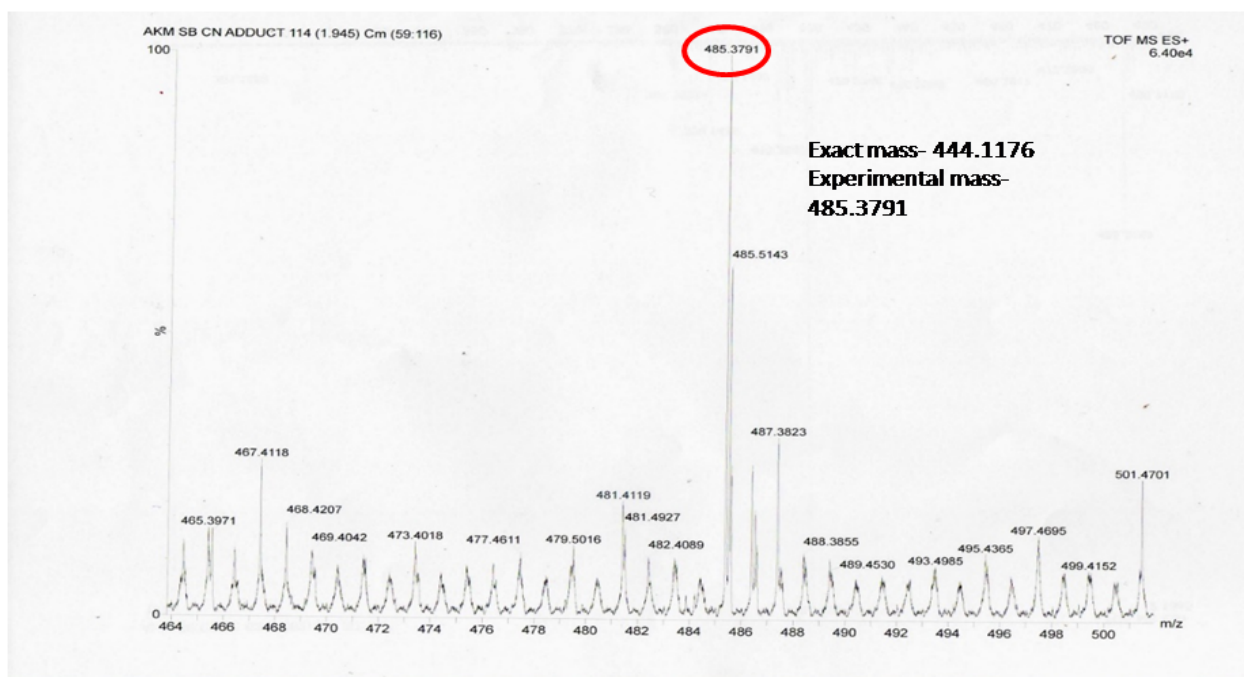


Figure S16: ESI-MS of product MNBTZ-CN [M+Na+H₂O]